Nuclear Physics B82 (1974) 172–188. North-Holland Publishing Company

# CONTRIBUTIONS OF MULTIPHOTON EXCHANGE IN ep DEEP INELASTIC SCATTERING

J. BARTELS *
*II. Institut für Theoretische Physik, Universität Hamburg*

Received 8 April 1974
(Revised 14 June 1974)

Abstract: An attempt is made, within a combined light-cone and parton approach, to estimate effects of multiphoton exchange in deep inelastic scattering. For the exchange of $n$ photons in the Bjorken limit, contributions of the form $(\ln^2 Q^2)^{n-1}$ times the one-photon approximation are found. Under the assumption that they are the leading ones in each order, they can be summed up to a power-behaved function of $Q^2$ which modifies the structure functions $W_i(\nu, Q^2)$ in such a way that in the Bjorken limit they are no longer functions only of $\omega$. A rough numerical estimate indicates that corrections due to multiphoton exchange become important (10% of the one-photon contribution) at about $Q^2 \sim 10^4$ GeV$^2$, but are always screened by the larger effect of radiative corrections at the electron vertex. They are, however, directly visible in $d\sigma(e^+p) - d\sigma(e^-p)$.

## 1. Introduction

Deep inelastic ep scattering has been considered in the one-photon approximation (fig. 1), and it is assumed that contributions of higher order (fig. 2) can be neglected when $Q^2 = -(k-k')^2$ is not very large. However, in the future larger values of $Q^2$ will

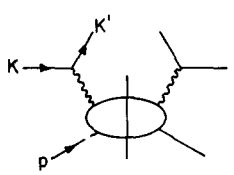


Fig. 1. One-photon approximation diagram.

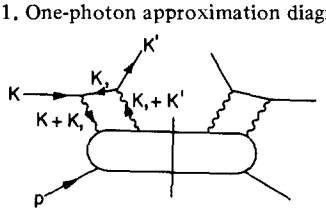


Fig. 2. Two-photon exchange contributions.

* Present address: National Accelerator Laboratory, Batavia, Illinois 60510, USA.

be accessible, and thus there may be some interest in a study of the contributions of two and more photons to deep inelastic ep scattering.

Kingsley [1] has made an estimate of two-photon effects, within the parton model of Landshoff, Polkinghorne and Short [2], and came to the conclusion that in fig. 2 there are contributions of the order $(\ln Q^2)^n$ in comparison to the one-photon approximation. The detailed form of this ln term, however, appeared to be dependent on one of the specific features of the parton model: the fall-off of the parton amplitudes as a function of the parton masses.

In the present paper we perform a study of two- (and more-) photon exchange in deep inelastic scattering, which as much as possible is based on the light-cone approach. At some points, however, we shall use parton model results as well. To explain our method we write down the amplitude of fig. 2:

$$\begin{aligned}\text{const}\ &[\int \mathrm{d}k_1\, \bar{u}(k')\gamma_\nu D_1 \gamma_\mu u(k) D_2 D_3]\ [\int \mathrm{d}k'_1\, \bar{u}(k')\gamma_{\nu'} D'_1 \gamma_{\mu'} u(k)\, D'_2 D'_3]^* \\ &\times \int \mathrm{d}x\mathrm{d}y_1\, \mathrm{d}y'_1 e^{iqx} e^{iy_1(k_1+\frac{1}{2}(k+k'))}\ e^{-iy'_1(k'_1+\frac{1}{2}(k+k'))} \qquad (1.1) \\ &\times \langle p|[T^*(J_{\nu'}(-\tfrac{1}{2}x+\tfrac{1}{2}y'_1)J_{\mu'}(-\tfrac{1}{2}x-\tfrac{1}{2}y'_1)),\ T(J_\mu(\tfrac{1}{2}x+\tfrac{1}{2}y_1)J_\nu(\tfrac{1}{2}x-\tfrac{1}{2}y_1))]|p\rangle\end{aligned}$$

(the momentum notation is contained in fig. 2; $D$ stands for the Feynman propagator). The hadronic part is represented by the matrix-element of four currents, and, apart from the integration over $k_1$ and $k'_1$, this expression occurs also in deep inelastic Compton scattering and deep inelastic electroproduction of massive muon pairs (fig. 3). This last process has been considered [3–5] by use of the bilocal algebra of Gell-Mann and Fritsch [6], and it was pointed out that in certain kinematical regions of the external photon momenta the leading contribution to the process is given by the singularities of the current product, all currents lying on one light-like vector in configuration space. In this region the bilocal algebra is expected to be valid, and its application relates the two-photon process of fig. 3 to the structure functions of the one-photon process fig. 1. The light cone part of the four-current product can be pictured by the quark parton diagram fig. 4. That the light-cone singularities are the most important ones means that other parton diagrams than that of fig. 4 are less important (e.g. fig. 5). All these considerations apply to products of currents with fixed large external photon momenta. In our case (1.1), however, the current momenta belong to loop integrals, and we have to find a way for handling the loop integral in the Bjorken limit (Bj-limit):

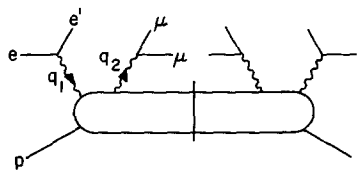


Fig. 3. Deep inelastic electroproduction of massive muon pairs.

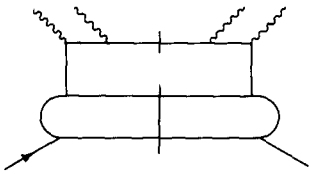

Fig. 4. Parton diagram which represents the light-cone part of the four-current product.

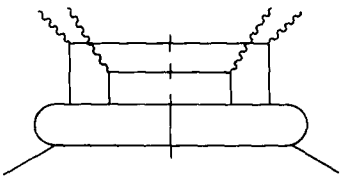

Fig. 5. Another parton diagram for the four-current product.

$$Q^2 = -q^2 - (k-k')^2 \to \infty, \quad \nu = p \cdot q \to \infty, \quad \omega = \frac{2\nu}{Q^2} \text{ fixed.} \tag{1.2}$$

From studies of the high-energy behavior of Feynman diagrams by means of Sudakov techniques [7] it is known that only certain subregions of the loop momentum integrations are responsible for the high-energy behavior, and one might expect that this is the case also for (1.1), because it differs from a usual Feynman diagram only by a $T$-product of full currents instead of a Feynman propagator. Furthermore, it is plausible that in the Bj-limit the photon momenta in (1.1) are somehow large and the light-cone (LC) singularities are important. If this is right, one arrives at the quark parton diagram of fig. 4 (the electron lines added), and can use the results on the asymptotic behavior of Feynman diagrams for the calculation of (1.1) in the Bj-limit. This is the method that we shall use in our paper. We isolate subregions of the loop integration and show the LC dominance for them. Then we use the bilocal algebra and arrive at a Feynman-like expression (fig. 4), multiplied by SU(3) structure functions, just as in ref. [3]. The remaining loop integrations, restricted to these subregions, give just a $\ln^2 Q^2$ times the one photon approximation (in fact, one $\ln^2 Q^2$ for each loop in fig. 2). In the same way we proceed for the multiphoton exchange, and when summing up these logarithms (including vertex corrections at the electron part, which also give rise to $\ln^2 Q^2$), we arrive at a power dependence on $Q^2$ for the overall deep inelastic process including multiphoton exchange:

$$(Q^2)^{-1+\text{const.}\sqrt{e^2/2\pi}} \cos(\text{const} \ln Q^2), \tag{1.3}$$

instead of $(Q^2)^{-1}$ for the single photon propagator in the one-photon approximation. For all this we use results on QED diagrams from Gribov et al. [8, 9]. A quantitative estimate of (1.3), however, shows that the corrections due to multiphoton exchange become important only for $Q^2 \gtrsim 10^4$ GeV$^2$.

In sect. 2 we consider the two-photon case, isolate the important momentum regions, discuss the LC dominance, and, by application of the bilocal algebra and the results of ref. [9], come to the $\ln^2 Q^2$. In the next section we extend this to more photons, and the last section is devoted to a discussion concerning the relevance of our results for present and future energies.

## 2. Two-photon contributions

As already mentioned in the introduction, we expect the LC contributions (fig. 4) to be important in the Bj-limit. Therefore, as a preparation, we consider the asymptotic behavior of the diagrams fig. 6a, b in the limit $Q^2 = -(k-k')^2 \to \infty$, $u = (r+r')^2$ fixed.

The wavy lines are photons, and for the moment we give them a mass $\lambda$ to avoid infrared divergencies. The solid lines belong to spin-$\frac{1}{2}$ particles. It is abvious that figs. 6a, b in the limit under consideration show the same behavior as figs. 7a, b respectively, in the limit $s = (k-k')^2 \to \infty$, "$t$" $= (r+r')^2$ fixed, when $s$ is replaced by $-Q^2$. This behavior has been studied in ref. [9], and the result is that fig. 7a behaves as

$$\frac{1}{2}\frac{\alpha}{2\pi}(\ln^2 s) f, \qquad (\alpha = e^2/2\pi)\,, \tag{2.1}$$

and fig. 7b as

$$2 \cdot \frac{1}{2}\,\frac{\alpha}{2\pi}(\ln^2 s) f, \tag{2.2}$$

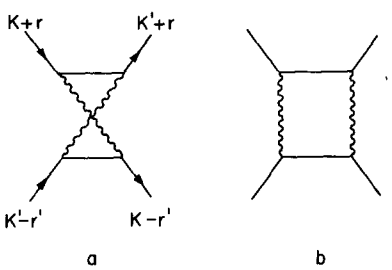


Fig. 6. Two-photon exchange between electron and parton in the Bjorken limit.

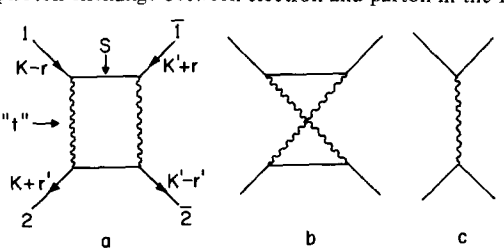


Fig. 7. Two-photon exchange in $e^+e^- \to \mu^+\mu^-$.

where $f$ is the amplitude for the Born approximation fig. 7c. By introduction of Sudakov variables

$$k_1 = \alpha k + \beta k' + k_{1\perp}, \qquad k_{1\perp} \cdot k = k_{1\perp} \cdot k' = 0 , \tag{2.3}$$

(we chose a reference frame where $k$, $k'$ are large and have only $z$-components), one can isolate the responsible integration regions. For fig. 7a the behavior (2.1) is due to those values of $k_1$, where both photons are off-shell and have large transverse momenta:

$$\frac{1}{s} < \alpha < 1, \frac{1}{s} < \beta < 1, \quad 1 \ll -k_{1\perp}^2 = s\alpha\beta. \tag{2.4}$$

In fig. 7b there are two regions: one of the photons carries the whole large momentum $k-k'$ and is far off-shell, whereas the other photon is real, both of them having large transverse components:

$$\frac{1}{s} < \alpha < 1, \quad \beta \sim 1, \quad 1 \ll -k_{1\perp}^2 = s\alpha\beta,$$

$$\frac{1}{s} < \beta < 1, \quad \alpha \sim 1, \quad 1 \ll -k_{1\perp}^2 = s\alpha\beta \tag{2.5}$$

[each of the regions contributes $\frac{1}{2}(\alpha/2\pi) f \ln^2 s$].

Now we return to fig. 2 and formula (1.1) and see whether we can find here such a $\ln^2 Q^2$, too. We take the proton rest frame, $k$ along the $z$-axis and are looking for the limit $Q^2 \sim \nu \to \infty$, $\omega$ fixed, and $\theta$ fixed ($\theta$ = scattering angle of the electron). This is equivalent to

$$-t = -(k-k')^2 = Q^2 \to \infty, \qquad s = (p+k)^2 \sim 2\nu \to \infty,$$

$$u = (p-k')^2 = M^2_{\text{nucleon}} \left(1 - \frac{2}{\omega(1-\cos\theta)}\right)^2 \tag{2.6}$$

($k'$ has finite components in our system). First we consider the region (2.4). Again, $k_1 = \alpha k + \beta k' + k_{1\perp}$, and the two photons have the momenta, according to fig. 2:

$$k_1 + k = (1+\alpha)\, k + \beta k' + k_{1\perp} \to (1+\alpha)\, k + \text{fixed vector}, \tag{2.7}$$

$$k_1 + k' = \alpha k + (1+\beta) k' + k_{1\perp} \to \alpha k + \text{fixed vector}. \tag{2.8}$$

Since $k'$ is finite and $|k_{1\perp}|$ is smaller than the two large components of $k$, both of (2.7) and (2.8) are nearly parallel to the large light-like vector $k$ (the electron mass may be assumed to be zero). Now we use the result of ref. [3]: if the momenta of the photons can be parametrized as $u_i e + b_i$ ($i = 1,2$; $u_i$ large numbers; $b_i$ fixed vectors; $e$ fixed light-like vector, common for both photons), then in the limit $u_i \to \infty$ the dominant contributions to the current product is given, when all currents are on one common light-like vector, and in this region the bilocal algebra is applicable.

For the region (2.5) the LC dominance is less obvious. Fritsch [3] has given arguments that for the two-photon deep inelastic process (fig. 3) with one or both photons being real and having small transverse momenta:

$$-(q_1-q_2)^2 \to \infty,\ 2pq_1 \to \infty,\quad 2pq_2 \to \infty,\qquad \xi = \frac{2p(q_1-q_2)}{-(q_1-q_2)^2} \text{ fixed}, \tag{2.9}$$

$q_1^2$ and/or $q_2^2 = 0$, $\quad q_{1\perp}^2$ and $q_{2\perp}^2$ small,

the leading LC contribution leads to a wrong behavior of the amplitude. But he argued that this could change, if the photon momenta $q_1$ and $q_2$ have large transverse components. Also in the parton model of Bjorken and Paschos [10] large transverse photon momenta enforce contributions with both photons attaching the same parton, in comparison with diagrams, where the photons interact with different partons. For the probability that a parton system, containing two partons with large transverse momenta, combines into one hadron goes faster to zero than the probablity for a process where both photons with large transverse momentum interact with the same parton and leave it without large transverse momentum. Furthermore, the LC dominance is also supported by the parton model of Landshoff et al. [2]. Kingsley [11] pointed out that for the two-photon process fig. 3 the disconnected diagram fig. 4 dominates the other parton diagrams, whenever the external invariants $(p+q_1)^2$, $(p-q_2)^2$ are large ($q_1^2$ and $q_2^2$ can be small or large). Summarizing all arguments, we conclude that there is strong evidence for region (2.5) to be LC dominated, and we shall use this in the following.

Having ensured that the conditions of validity of the bilocal algebra of Gell-Mann and Fritsch are fulfilled we calculate the LC part of (1.1): the hadronic part of (1.1) is:

$$\int \mathrm{d}^4x\, \mathrm{e}^{iqx} \int \mathrm{d}^4y_1\, \mathrm{d}^4y_1'\, \mathrm{e}^{iy_1(k_1+\frac{1}{2}(k+k'))}\, \mathrm{e}^{-iy_1'(k_1'+\frac{1}{2}(k+k'))} \tag{2.10}$$

$$\times \langle p|[T^*(J_\rho(-\tfrac{1}{2}x+\tfrac{1}{2}y_1')J_\sigma(-\tfrac{1}{2}x-\tfrac{1}{2}y_1')),\ T(J_\nu(\tfrac{1}{2}x+\tfrac{1}{2}y_1)J_\mu(\tfrac{1}{2}x-\tfrac{1}{2}y_1))]\,|p\rangle.$$

With the notations:

$$J_\mu(x) = \bar{\psi}(x)\,\gamma_\mu Q \psi(x),$$

$$Q = \tfrac{1}{2}(\lambda_3 + \sqrt{\tfrac{1}{3}}\,\lambda_8),$$

$$J_{\mu\pm}^i(x,y) = \bar{\psi}(x)\gamma_\mu\, \tfrac{1}{2}\lambda_i\, \bar{\psi}(y) \pm \psi(y)\,\gamma_\mu\, \tfrac{1}{2}\lambda_i\, \psi(x), \tag{2.11}$$

(where $\lambda_i$ are the SU(3) matrices) the LC part of (2.10) is just the quark parton line in fig. 8 with formal massless quarks:

$$tr\left[\frac{1}{\omega}\hat{p}\,\gamma_\mu \frac{\hat{k}_1+\hat{k}+\hat{p}/\omega}{(k_1+k+p/\omega)^2+i\epsilon}\,\gamma_\nu(\hat{p}/\omega+\hat{q})\gamma_\sigma \frac{\hat{k}_1'+\hat{k}+p/\omega}{(k_1'+k+p/\omega)^2-i\epsilon}\,\gamma_\rho\right], \tag{2.12}$$

$(\hat{p} = p\cdot\gamma)$,

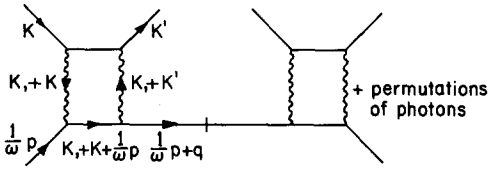


Fig. 8. Light cone part of (2.10).

and similar expressions for the other permutations of the photon lines on both sides of the diagram. (2.12) has still to be multiplied by a term that reflects the SU(3) content of the four current product. With the identity:

$$Q^4 = (\tfrac{2}{3})^4[\sqrt{\tfrac{2}{3}}\,\tfrac{1}{2}\lambda_0 + \tfrac{1}{2}\lambda_3 + \sqrt{\tfrac{1}{3}}\,\tfrac{1}{2}\lambda_8] + (-\tfrac{1}{3})^4[2\sqrt{\tfrac{2}{3}}\tfrac{1}{2}\lambda_0 - \tfrac{1}{2}\lambda_3 - \sqrt{\tfrac{1}{3}}\,\tfrac{1}{2}\lambda_8], \quad (2.13)$$

we obtain for the SU(3) decomposition:

$$\begin{aligned}&(\tfrac{2}{3})^4[\sqrt{\tfrac{2}{3}}\,G^0_-(1/\omega) + G^3_-(1/\omega) + \sqrt{\tfrac{1}{3}}\,G^8_-(1/\omega)]\\ &\quad + (-\tfrac{1}{3})^4[2\sqrt{\tfrac{2}{3}}\,G^0_-(1/\omega) - G^3_-(1/\omega) - \sqrt{\tfrac{1}{3}}\,G^8_-(1/\omega)]\\ &\quad = (\tfrac{2}{3})^4 A_1(\omega) + (-\tfrac{1}{3})^4 A_2(\omega)\,, \end{aligned} \quad (2.14)$$

with the structure functions $G^i_\pm(\xi)$ defined by:

$$\langle p|J^i_{\mu\pm}(x,0)|p\rangle = p_\mu \int d\xi\, e^{i\xi p\cdot x}\, G^i_\pm(\xi) + \text{terms prop. } x_\mu \quad (2.15)$$

(axial currents do not appear in our result (2.14), because they drop out after averaging over the target spin).

Now fig. 8 is a product of two Feynman diagrams, and it is easy to see that in the Bj-limit we can just use our results (2.1) and (2.2). Thus the asymptotic behavior of fig. 8 (the LC part of fig. 2) is:

$$\begin{aligned}&L_{\mu\rho}\left(\frac{e^2}{Q^2}\right)^2 \left(-\frac{3}{4}\frac{\alpha}{\pi}\ln^2 Q^2\right)^2 \pi r\left[\frac{1}{\omega}\hat{p}\,\gamma_\mu\left(\frac{1}{\omega}\hat{p}+\hat{q}\right)\gamma_\rho\right]\\ &\quad \times \frac{\pi}{2Q^2}\,[(\tfrac{2}{3})^4 A_1(\omega) + (-\tfrac{1}{3})^4 A_2(\omega)]. \end{aligned} \quad (2.16)$$

($L_{\mu\rho}$ stands for the leptonic part, the trace of the electron spinors.) For comparison, we write down the one-photon approximation (fig. 1):

$$L_{\mu\rho}\left(\frac{e^2}{Q^2}\right)^2 \pi r\left[\frac{1}{\omega}\hat{p}\,\gamma_\mu\left(\frac{1}{\omega}\hat{p}+\hat{q}\right)\gamma_\rho\right]\frac{\pi}{2Q^2}\,[(\tfrac{2}{3})^2 A_1(\omega) + (-\tfrac{1}{3})^2 A_2(\omega)]. \quad (2.17)$$

By comparison of (2.16) and (2.17) one verifies that the two-photon term is essentially the one photon part, multiplied by a $\ln^2 Q^2$.

To summarize our result, we have isolated two regions of the loop integration in fig. 2, where the light cone is of importance, and its contribution yields an enhancement $\ln^2 Q^2$, compared with the one-photon approximation. We cannot exclude that other parts of the integration could equally lead to such logarithmic factors. If they exist, they are not light-cone dominated, because we have picked up the leading term of the quark parton diagram fig. 8. Within the parton model of Landshoff et al., Kingsley [1] found only two regions, which are important in the Bj-limit, and they are the same as ours. For the rest of the paper, we shall assume that there are no other contributions that give rise to $\ln^2 Q^2$ or even more. With these assumptions, we can treat also the exchange of three and more photons. This will be done in sect. 3.

In order to complete our discussion of two-photon exchange contributions, we still have to study the interference diagram (fig. 9): In this diagram the photon states on the right- and left-hand side have different behavior under charge conjugation, and, as a consequence of this, we obtain in the Bj limit for fig. 9:

$$L_{\mu\rho}\left(\frac{e^2}{Q^2}\right)^2\left(-\frac{3}{4}\frac{\alpha}{\pi}\ln^2 Q^2\right)\tau r\left[\frac{1}{\omega}\hat{p}\,\gamma_\mu\left(\frac{1}{\omega}\hat{p}+\hat{q}\right)\gamma_\rho\right]$$

$$\times\frac{\pi}{2Q^2}\left[(\tfrac{2}{3})^3 S_1(\omega)+(-\tfrac{1}{3})^3 S_2(\omega)\right]. \tag{2.18}$$

Here the SU(3) decomposition contains matrixelements of the symmetric bilocal operators cf. (2.14)]:

$$S_1(\omega)=\sqrt{\tfrac{2}{3}}\,G_+^0(1/\omega)+G_+^3(1/\omega)+\sqrt{\tfrac{1}{3}}\,G_+^8(1/\omega),$$

$$S_2(\omega)=2\sqrt{\tfrac{2}{3}}\,G_+^0(1/\omega)-G_+^3(1/\omega)-\sqrt{\tfrac{1}{3}}\,G_+^8(1/\omega). \tag{2.19}$$

In sect. 4 we discuss how to get an estimate of the $A_i$ and $S_i$.

## 3. Generalization to many-photon exchange

In the general case (fig. 10) of $n$ photons between electron and hadronic part we have to consider seperately four classes of diagrams, according to the charge conjugation properties of the photon systems. By (+, +), we denote the amplitudes, where on both sides there is an even number of photons ($C = +$), and the analog holds for the three other cases (−, −), (+, −) and (−, +). For (+, +) and (−, −) the SU(3) de-

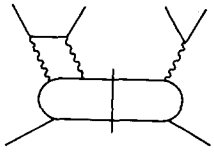

Fig. 9. Interference diagram in ep-deep inelastic scattering.

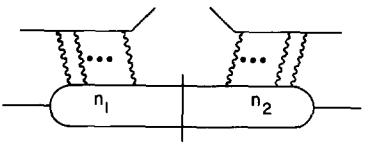


Fig. 10. n-photon exchange contribution.

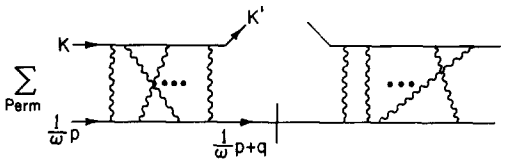


Fig. 11. LC-part of fig. 10.

composition is

$$(\tfrac{2}{3})^{n_1+n_2} A_1(\omega) + (-\tfrac{1}{3})^{n_1+n_2} A_2(\omega) \ , \tag{3.1}$$

and for the interference terms (+, −), (−, +):

$$(\tfrac{2}{3})^{n_1+n_2} S_1(\omega) + (-\tfrac{1}{3})^{n_1+n_2} S_2(\omega). \tag{3.2}$$

Taking only the leading LC singularities in the multiple current product of the hadronic part of fig. 10, we obtain, just as in sect. 2, the quark parton diagram fig. 11 with massless quarks: Here the sum has to be taken over all possible crossings of the photons on both sides. For large $Q^2$ (i.e. the Bj-limit) the asymptotic behavior can be calculated, as in sect. 4, by use of ref. [9]. The diagram behaves as:

$$\frac{1}{Q^2} \ (\ln^2 Q^2)^{n_1-1} \ \frac{1}{Q^2} \ (\ln^2 Q^2)^{n_2-1} , \tag{3.3}$$

and this behavior is determined by those regions of momentum integration, where at least one photon on each side is highly virtual. Furthermore, all photon momenta have large transverse components. Thus we can apply the arguments of sect. 2 to show LC dominance.

Before we take the sum over $n_1$ and $n_2$ (seperately for even and odd values), we still add to fig. 10 all possible vertex corrections along the electron lines. It is known [12] that they also contain $\ln^2 Q^2$ terms. As to the hadronic side, it is not quite clear, neither from the point of view of light-cone dominance nor within the parton model of Bjorken and Paschos, how to calculate electromagnetic corrections. Kingsley [1] has tried to include them into his analysis within the softened parton model. He argued that there might be logarithmic renormalization effects within the hadronic part, but he did not determine them. In our study, we make no attempt to examine this point in further detail. Vertex corrections along the parton line might be part of electromagnetic corrections, and they would give contributions $\ln^2 Q^2$ just as at

the electron vertex. However, in our final result which we shall write down in a moment they would not affect the general form but only modify the value of certain parameters. The same will probably hold for other electromagnetic corrections on the hadronic side. For consistency we shall omit the vertex corrections along the parton line, having in our mind that our result will not represent all sorts of higher order electromagnetic effects, but only those on the electron side and those between electron and hadronic part.

Calculating now the sum of all diagrams (details of how to derive our results from ref. [9] are given in the appendix), we obtain for the different charge conjugation parts:

$$(+,+)\quad L_{\mu\rho}\left(\frac{e^2}{Q^2}\right)^2 tr\left[\frac{1}{\omega}\hat{p}\,\gamma_\mu\left(\frac{1}{\omega}\,\hat{p}+\hat{q}\right)\gamma_\nu\right]$$

$$\times\frac{\pi}{2Q^2}\,[(\tfrac{2}{3})^2 A_1(\omega)\,F_{1+}^2(Q^2)+(-\tfrac{1}{3})^2 A_2(\omega)\,F_{2+}^2(Q^2)], \tag{3.4a}$$

$$(-,-)\quad L_{\mu\rho}\left(\frac{e^2}{Q^2}\right)^2 tr\left[\frac{1}{\omega}\hat{p}\,\gamma_\mu\left(\frac{1}{\omega}\hat{p}+\hat{q}\right)\gamma_\rho\right]$$

$$\times\frac{\pi}{2Q^2}\,[(\tfrac{2}{3})^2 A_1(\omega)\,F_{1-}^2(Q^2)+(-\tfrac{1}{3})^2 A_2(\omega)F_{2-}^2(Q^2)], \tag{3.4b}$$

$$(+,-)=(-,+)\quad L_{\mu\rho}\left(\frac{e^2}{Q^2}\right)^2 tr\left[\frac{1}{\omega}\hat{p}\gamma_\mu\left(\frac{1}{\omega}\hat{p}+\hat{q}\right)\gamma_\rho\right] \tag{3.4c}$$

$$\times\frac{\pi}{2Q^2}\,[(\tfrac{2}{3})^2 S_1(\omega)\,F_{1+}(Q^2)\,F_{1-}(Q^2)+(-\tfrac{1}{3})^2 S_2(\omega)\,F_{2+}(Q^2)\,F_{2-}(Q^2)].$$

The functions $F_{i\pm}(Q^2)$ are also given in more detail in the appendix. Here we show only the first terms of the low energy expansion (for the case that vertex corrections on the parton line are emitted):

$$F_{1+}(Q^2)=-\frac{\alpha}{2\pi}\ln^2 Q^2+\frac{34}{72}\left(\frac{\alpha}{2\pi}\right)^2\ln^4 Q^2\pm\ldots, \tag{3.5a}$$

$$F_{1-}(Q^2)=1-\frac{\alpha}{4\pi}\ln^2 Q^2+\frac{41}{72}\left(\frac{\alpha}{2\pi}\right)^2\ln^4 Q^2\pm\ldots, \tag{3.5b}$$

$$F_{2+}(Q^2)=-\frac{\alpha}{2\pi}\ln^2 Q^2-\frac{17}{24}\left(\frac{\alpha}{2\pi}\right)^2\ln^4 Q^2\pm\ldots, \tag{3.5c}$$

$$F_{2-}(Q^2)=1-\frac{\alpha}{4\pi}\ln^2 Q^2+\frac{17}{24}\left(\frac{\alpha}{2\pi}\right)^2\ln^4 Q^2\pm\ldots, \tag{3.5d}$$

and the behavior for large $Q^2$:

$$F_{i\pm}(Q^2 \sim \text{const.}\cosh(\sqrt{\alpha/2\pi}\, x \ln Q^2)\cos(\sqrt{\alpha/2\pi}\, y \ln Q^2)$$
$$\sim \text{const.}\,(Q^2)^{x\sqrt{\alpha/2\pi}}\cos(\sqrt{\alpha/2\pi}\, y \ln Q^2). \tag{3.6}$$

The parameters $x$, $y$ are found according to the description in the appendix, and we give no numerical values for them, because (3.6) is to be considered only as a qualitative result. We shall discuss this in sect. 4. In the low-$Q^2$ expansion (3.5) one verifies that the lowest terms, inserted into (3.4), reproduce the contributions of figs. 1, 2 and 9.

For the differential cross section of ep deep inelastic scattering we add (+, +), (−, −), (−, +) and (+, −) terms, and after the decomposition of the trace term into

$$tr\left[\frac{1}{\omega}\hat{p}\gamma_\mu\left(\frac{1}{\omega}\hat{p}+\hat{q}\right)\gamma_\nu\right] = 2Q^2\left[-\left(g_{\mu\nu}-\frac{q_\mu q_\nu}{q^2}\right)\right.$$
$$\left.+\frac{2}{\omega\nu}\left(p_\mu-\frac{pq}{q^2}q_\mu\right)\left(p_\nu-\frac{pq}{q^2}q_\nu\right)\right], \tag{3.7}$$

we obtain for the structure functions $W_1(\nu, q^2)$ and $W_2(\nu, q^2)$ in the Bj-limit:

$$W_1(\nu, q^2) = \frac{1}{\omega}\left\{(\tfrac{2}{3})^2 A_1(\omega)[F_{1+}^2(Q^2)+F_{1-}^2(Q^2)] + (\tfrac{2}{3})^2 2S_1(\omega)\, F_{1+}(Q^2)F_{1-}(Q^2)\right.$$
$$\left.+(-\tfrac{1}{3})^2 A_2(\omega)[F_{2+}^2(Q^2)+F_{2-}^2(Q^2)] + (-\tfrac{1}{3})^2 2S_2(\omega)\, F_{2+}(Q^2)\, F_{2-}(Q^2)\right\},$$
$$W_2(\nu, q^2) = \frac{2}{\omega\nu} M_{\text{nucl}}^2\, W_1(\nu, q^2). \tag{3.8}$$

This has to be compared with the one-photon approximation:

$$W_1(\nu, q^2) = \frac{1}{\omega}\left\{(\tfrac{2}{3})^2 A_1(\omega) + (-\tfrac{1}{3})^2 A_2(\omega)\right\}. \tag{3.9}$$

## 4. Results and discussion

The result of our considerations is contained in (3.8) and states that in the Bj-limit (for very large $Q^2$) $W_1(\nu, q^2)$ is not simply a function of $\omega$ (as it was the case in the one-photon approximation). The $Q^2$ dependence, however, is completely contained in the $F_{i+}(Q^2)$, which for small $Q^2$ are almost 1 or zero and for large $Q^2$ have a power dependence on $Q^2$.

For practical use one needs a quantitative estimate of the multiphoton influence. For this we have to know the functions $S_i$ and $A_i$ and the scale mass of $Q^2$ in the $F_{i\pm}(Q^2)$. In the previous sections we have always, for simplicity, written: $\ln^2 Q^2$,

but there is, of course, still a scale mass in the logarithm: $\ln^2(Q^2/m^2)$, and for numerical statements we have to take care of this mass.

First we look at the functions $S_i$ and $A_i$. Three of them, $A_1$, $A_2$ and $S_1$ can be expressed by structure functions of deep inelastic ep, en, $\nu$p, and $\nu$n scattering:

$$A_1(\omega) = \sqrt{\tfrac{2}{3}}\, G_-^0(1/\omega) + G_-^3(1/\omega) + \sqrt{\tfrac{1}{3}}\, G_-^8(1/\omega)$$

$$= \omega[3F_2^{ep} - \tfrac{2}{3}(F_2^{ep} + F_2^{en}) + \tfrac{1}{4}(F_2^{\nu p} + F_2^{\nu n})], \tag{4.1}$$

$$A_2(\omega) = 2\sqrt{\tfrac{2}{3}}\, G_-^0(1/\omega) - G_-^3(1/\omega) - \sqrt{\tfrac{1}{3}}\, G_-^8(1/\omega)$$

$$= \omega[-3F_2^{ep} + 2(F_2^{ep} + F_2^{en}) - \tfrac{3}{4}(F_2^{\nu p} + F_2^{\nu n})], \tag{4.2}$$

$$S_1(\omega) = \sqrt{\tfrac{2}{3}}\, G_+^0(1/\omega) + G_+^3(1/\omega) + \sqrt{\tfrac{1}{3}}\, G_+^8(1/\omega)$$

$$= \frac{1}{4}(F_3^{\nu p} + F_3^{\nu n}) + \tfrac{1}{4}\omega(F_2^{\nu p} - F_2^{\nu n}). \tag{4.3}$$

The remaining function $S_2$ cannot be built up in this way. Thus we must use model-dependent assumptions for an estimate. In the quark parton model ($x = 1/\omega$, $M$ nucleon mass):

$$A_1(\omega) = \frac{1}{2Mx}(u(x) + \bar{u}(x)), \quad A_2(\omega) = \frac{1}{2Mx}(d(x) + \bar{d}(x) + s(x) + \bar{s}(x)), \tag{4.4}$$

$$S_1(\omega) = \frac{1}{2Mx}(u(x) - \bar{u}(x)), \qquad S_2(\omega) = \frac{1}{2Mx}(d(x) - \bar{d}(x) + s(x) - \bar{s}(x)),$$

where $u$, $\bar{u}$, $d$, $\bar{d}$, $s$, $\bar{s}$ are the momentum distributions of the quarks and antiquarks. Under the assumption that antiquarks are not important we expect that the functions $S_i$ are of the same order of magnitude as the $A_i$. The validity of this can be checked be comparison of the experimental values of (4.3) and (4.1).

We finally come to the question, for which values of $Q^2$ the functions $F_i(Q^2)$ can no longer be approximated by their low energy limits 1 (for $F_{i-}$) and zero (for $F_{i+}$). This will be the case, when the first term $\ln^2 Q^2$ in the expressions (3.5) are not negligible, and at the same time this gives also a condition on the range of validity of our approximation methods. For each power of $\alpha$ we have taken into account only the leading term $(\ln^2 Q^2)^n$, and this is justified only when the leading term is larger than the next one.

In this discussion we also have to take care of the infrared problem. In sect. II we have seen that the integration regions, which determine the leading $\ln^2 Q^2$ term, contain real photons and are thus under the influence of infrared divergencies. For this reason we introduced the photon mass $\lambda$, and our final result (3.8) still depends on it. In order to obtain a result free from infrared divergencies and photon mass, we have to add to the diagrams with virtual infrared photons still those with bremsstrahlung [13], and only the sum of both can be considered as a quantitative

result. For a treatment of the bremsstrahlung, however, there are difficulties. The bremsstrahlung contributions also contains $\ln^2 Q^2$ terms (which can be calculated in the same way as the logarithms of the last sections, because they involve large transverse momenta of the photons), and in part they cancel those of the virtual photons of the last sections. Because of this cancellation one needs, besides the terms $\ln^2 Q^2$, also the next leading contributions, and for their calculation a method has to be found how to treat, e.g., the interaction of soft photons with the final hadron states ("anything"). Because of this unresolved problem we do not try to take into account bremsstrahlung in all orders, and our result (3.5) of the previous section describes only qualitatively the influence of many-photon contributions. For the rest of our paper, we only try to find an estimate of the lowest order corrections $\sim \alpha$, the two-photon contributions.

For these we found three terms that contribute: the regions (2.4), (2.5) and the vertex correction in lowest order at the electron vertex (we omit those of the parton line). In region (2.4) both photons have a large mass, and the photon mass $\lambda$ plays no role in this contribution. The parton line in Fig. 8 was massless, as a consequence of our LC approach, and since the electron mass is the only mass in the diagram, we obtain $(\ln(Q^2/\text{electron mass}^2))^2$. Thus the contribution of region (2.4), relatively to the one-photon approximation,

$$2\left(\text{parton charge } \frac{2}{3}\right)\frac{1}{2}\frac{\alpha}{2\alpha}\ln^2\frac{Q^2}{m_e^2}, \tag{4.5}$$

is about $\frac{2}{10}$ already at $Q^2 \sim 3$ GeV$^2$, and if the pure LC approach is correct, one should see the influence of two photons already at present energies. On the other hand, if we use a parton picture and give the parton a mass $m_{\text{parton}}$, which at any rate will be much larger than the electron mass $m_e$, then we have two masses in the diagram. But the electron mass is zero in comparison with the parton mass, and the logarithmic term will contain the parton mass. For $m_{\text{parton}} = 1$ GeV, (4.5) reaches the value $\frac{1}{10}$ at $Q^2 \sim 10^5$ GeV$^2$, for $m_{\text{parton}} = 0.3$ GeV at $Q^2 \sim 10^3$ GeV$^2$. Now we consider the vertex corrections at the electron vertex together with the corresponding bremsstrahlung diagrams (fig. 12).

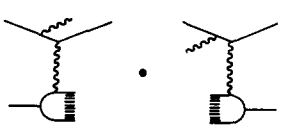

Fig. 12. Bremsstrahlung at the electron vertex.

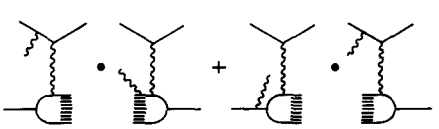

Fig. 13. Bremsstrahlung between eleectron and hadron.

Both of them contain terms $\ln^2(Q^2/m_e^2)$, but they cancel each other. For the calculation of the remaining terms we take, as an approximation, for the final hadron state the lowest mass, the nucleon mass $M$, and then use ref. [14], where ep elastic scattering together with bremsstrahlung is studied in detail. According to this, we obtain, for the electron vertex correction and bremsstrahlung of fig. 12:

$$\frac{\alpha}{\pi}\left\{\ln\frac{Q^2}{m_e^2}\left[2\ln\frac{E}{\Delta E}-3\ln\left(\frac{Q^2}{M^2}\,\frac{\omega^2}{4}(1-\cos\theta)\right)\right]+\frac{1}{2}\ln^2\left(\frac{Q^2}{M^2}\,\frac{\omega^2}{4}(1-\cos\theta)\right)\right\} \tag{4.6}$$

($\Delta E$ is the limit of Bremsstrahlung energy, $E$ the energy of the incoming electron, $M$ nucleon mass, $m_e$ electron mass). If $E/\Delta E$ is large but fixed when $E$ is increasing, the second and third term in (4.6) grow faster than the first and will dominate for large $Q^2$. When we take $E/\Delta E$ of the order 100, $1-\cos\theta \sim 0.1$, $\frac{1}{4}\omega^2 \sim 1$, then the first term will dominate up to $Q^2 \lesssim 10^3$ GeV$^2$ and yield an effect up to 50%. For larger values, $Q^2 \gtrsim 10^4$ GeV$^2$, the second term will dominate, and (4.6) grows as

$$\frac{3\alpha}{\pi}\ln\frac{Q^2}{m_e^2}\ln\left(\frac{Q^2}{M^2}\,\frac{\omega^2}{4}(1-\cos\theta)\right). \tag{4.7}$$

In the regions (2.5) of the two-photon exchange one photon is in the infrared region, and we have to add the bremsstrahlung diagrams of fig. 13. In order to obtain an estimate of their sum we have to find a way to treat the bremsstrahlung at the hadronic vertex. For simplicity, we assume that the most important contributions are due to the nucleon in the final state and than use again ref. 14. There we find that the sum of fig. 13 and the two-photon exchange contains terms of the form

$$\frac{\alpha}{2\pi}\ln^2\frac{Q^2}{M^2}\,, \tag{4.8}$$

but no logarithms with the electron mass in den denominator. (4.8) will be of the order $\frac{1}{10}$ at about $Q^2 \gtrsim 10^4$ GeV$^2$.

Summarizing what we have found for the influence of two-photon effects, we expect that for $Q^2$ up to $10^4$ GeV$^2$ the main contributions will be due to the first term in (4.6), i.e. the radiative corrections at the electron vertex. The influence of two-photon exchange will be small. For larger $Q^2$, the radiative corrections continue to yield the largest effect, but in the two-photon exchange there are now contributions (4.5) and (4.8), which are no longer negligible in comparison with the one-photon approximation ($\geqslant 10\%$). To make them visible one either has to subtract in ep deep inelastic the radiative corrections of the leptonic vertex or to use data of $e^+p$ and $e^-p$ deep-inelastic scattering, because the lowest order contribution to $d\sigma(e^+p) - d\sigma(e^-p)$ is just the interference diagram fig. 9. On the ground of our estimate we expect, that this diagram will be 10% of the one photon approximation at $Q^2 \sim 10^4$ GeV$^2$. For a precise prediction of the behavior of the ep deep inelastic cross section as a function of $Q^2$ at large values of $Q^2$, a detailed study of brems-

strahlung in this process is necessary. Our considerations show that, for $Q^2 \gtrsim 10^4$ GeV$^2$, multiphoton exchange together with radiative corrections and bremsstrahlung ($E/\Delta E$ is assumed to be fixed when $Q^2$ is increased) yield some power behavior of $Q^2$, multiplied by a bounded function of $Q^2$, such as in (3.8).

*Note added.* After having finished this paper we learned about a study of P. Fishbane and R. Kingsley on the same subject (Phys. Rev. D8 (1973) 3074). They examined the contributions due to the exchange of two photons, and their results qualitatively agree with ours. In the numerical estimate of the value $Q^2$, for which the two-photon contributions reach 10% of the one-photon approximation, we disagree. They estimate $Q^2$ to be of the order 20 GeV$^2$, which is the value for which $\alpha \ln^2(Q^2/m_\rho^2) = \frac{1}{10}$. However, we find that the ratio of the two-photon term to the one-photon part is $(\alpha/2\pi) \ln^2(Q^2)$, and since $Q^2$ appears only as logarithm, the actual value of $Q^2$ depends strongly on this factor $1/2\pi$. This explains our disagreement. We also have chosen another scale mass, but this accounts only for a factor $\frac{1}{2}$ for $Q^2$.

I am indebted to Professor G. Kramer for suggestions and useful discussions, Dr. T. Walsh and Dr. W. Bartel for very helpful comments. The results on QED asymptotics I learned during a stay at the Leningrad Institute of Nuclear Research and I would like to express my gratitude to Professor V.N. Gribov and Dr. L.N. Lipatov.

## Appendix

The results of ref. [9] can be summarized in the following way. For the process $1\bar{1} \to 2\bar{2}$ (fig. 14) with particles 1 and 2 having charges e and e′ (in units of the negative electron charge), the amplitude at $s$ large, $t$ fixed takes the form (photons with mass $\lambda$):

$$T_{e,e'} = f \frac{1}{2\pi i} \int_{c-i\infty}^{c+i\infty} \mathrm{d}z \cosh(z\sqrt{\gamma} \ln s)\, \varphi(z) \frac{D'_{-\beta}(z)}{D_{-\beta}(z)} \quad , \qquad \text{(A.1)}^*$$

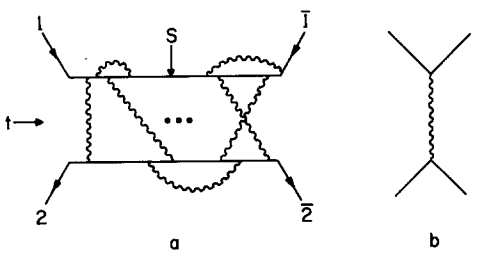


Fig. 14. (a) General contribution to the process $1\bar{1} \to 2\bar{2}$. (b) Lowest order diagram.

* Formula (A.1) is taken from ref. [9], but the solution given there in (II.11) is not quite correct. Instead of $\exp(z\gamma\rho)$, there has to be a $\cosh(z\gamma\rho)$. As given in ref. [9], the solution is not symmetric under $\rho \to -\rho$, as it should be. It also does not satisfy the boundary condition (II.2). Furthermore, since we have given the photon a mass $\lambda$, all contributions in ref. [9] with $k_\perp^2 \ll 1$ are omitted.

where $f$ is the amplitude for the Born approximation (fig. 14b), $D_n$ the parabolic cylinder functions of order $n$ and the parameters $\beta$, $\gamma$ have the meaning:

$$\gamma = \frac{\alpha}{2\pi}(-2ee' + e^2 + e'^2), \tag{A.2}$$

$$\beta = \frac{\alpha}{2\pi}\frac{-ee'}{\gamma}. \tag{A.3}$$

In (A.2) the second and the third term $e^2$ and $e'^2$ are due to the radiative (vertex) corrections for particle 1 and 2, and they have to be omitted if radiative corrections are not taken into account. For $e = e'$, $\gamma$ can be zero, and in this case (A.1) is not valid, but one has to use the result of ref. [8]. (A.1) is a Sommerfeld-Watson integral and is determined by the singularities of the integrand. $\phi(z)$ is an entire function, and constraints on it are imposed by (II.2) of the appendix of ref. [9]. From this it follows:

$$1 = \frac{1}{2\pi i}\int_{c-i\infty}^{c+i\infty}\left[dz\ \ \varphi(z)\frac{\frac{d}{dz}H_{-\beta}(z+\xi)}{2H_{-\beta}(z)} + \varphi(-z)\frac{\frac{d}{dz}H_{-\beta}(-z-\xi)}{2H_{-\beta}(-z)}\right], \tag{A.4}$$

$$H_{-\beta}(z) = e^{-\frac{1}{4}z^2}D_{-\beta}(z), \qquad \xi = \ln s.$$

The cylinder functions $D_n$ have a finite number of simple zeros. For large values of $\ln s$, in (A.1) only the two complex conjugate poles $z_k$ and $\bar{z}_k$ with the largest real part are important:

$$\begin{aligned} T &\sim f\varphi(z_k)\cosh(\mathrm{Re}\, z_k\sqrt{\gamma}\ln s)\cos(\mathrm{Im}\, z_k\sqrt{\gamma}\ln s) \\ &\sim f\varphi(z_k)\tfrac{1}{2}s^{\mathrm{Re}z_k\sqrt{\gamma}}\cos(\mathrm{Im}\, z_k\sqrt{\gamma}\ln s). \end{aligned} \tag{A.5}$$

If in (A.1) $\gamma < 0$ we have to interchange in (A.5) Re $(z_k)$ and Im $(z_k)$ and to take the zero with the largest imaginary part. For small values of $\ln s$ we have the expansion:

$$T = f\left[1 - \frac{\ln^2 s}{2!}\gamma(1+\beta) + \frac{\ln^4 s}{4!}\gamma^2(1+\beta)(3+2\beta) \pm \ldots\right]. \tag{A.6}$$

To derive from this our results (3.5) and (3.6) we have to have in mind that our process is $e^-e^+ \to$ parton + antiparton with energy $q^2 = -Q^2$, the partons having charges $\frac{2}{3}$ and $-\frac{1}{3}$. Thus $e = -1$ and $e' = \frac{2}{3}\ (-\frac{1}{3})$ in (A.2) Finally, we have to consider seperately even and odd numbers of photons between electron and parton. This is achieved by taking instead of $T_{e,e'}$, the even and odd combinations $\frac{1}{2}(T_{e,e'} \pm T_{e,-e'})$.

## References

[1] R.L. Kingsley, Nucl. Phys. 46B (1972) 615.
[2] P.V. Landshoff, J.C. Polkinghorne and R.D. Short, Nucl. Phys. 28B (1971) 225;
P.V. Landshoff and J.C. Polkinghorne, Phys. Reports 5 (1972) 1.

[3] H. Fritsch, CERN ref. TH. 1489.
[4] M. Chaichian, Nucl. Phys. 42B (1972) 333.
[5] J. Iliopoulos and E.A. Paschos, NAL-THY-48
[6] H. Fritsch and M. Gell-Mann, Procs. of the Coral Gable Conf., 1971.
[7] V.V. Sudakov, JETP (Sov.Phys.) 30 (1956) 87.
[8] V.G. Gorshkov, V.N. Gribov, L.N. Lipatov and G.V. Frolov, Yad, Phys. (USSR) 6 (1967) 129.
[9] V.G. Gorshkov, V.N. Gribov, L.N. Lipatov and G.V. Frolov, Yad. Phys. (USSR) 6 (1967) 361.
[10] J.D. Bjorken and E.A. Paschos, Phys. Rev. 185 (1969) 1975.
[11] R.L. Kingsley, Nucl. Phys. 52B (1973) 203.
[12] R. Jackiw, Ann. of Phys. 48 (1968) 292;
P.M. Fishbane and J.D. Sullivan, Phys. Rev. D4 (1971) 458.
[13] D.R. Yennie, S.C. Frautschi and H. Suura, Ann. of Phys. 13 (1961) 379.
[14] Y.-S. Tsai, Phys. Rev. 122 (1961) 1898.